Scientia Iranica B (2023) 30(6), 1973–1986

Sharif University of Technology
**Scientia Iranica**
*Transactions B: Mechanical Engineering*
http://scientiairanica.sharif.edu

# Effect of the magnetic field of a current-carrying conductor on the vibrations of magnetoelastic plate structures

**M. Nasrabadi[a], A. Ghaffari[b], B. Heydari[b], and A. Afkar[c,*]**

a. *Department of Mechanical Engineering, Islamic Azad University, Karaj Branch, Karaj, Iran.*
b. *Department of Mechanical Engineering, Islamic Azad University, Shabestar Branch, Shabestar, Iran.*
c. *Department of Vehicle Engineering, Technology and Engineering Research Center, Standard Research Institute, Iran.*

Received 4 June 2022; received in revised form 10 December 2022; accepted 5 February 2023

**KEYWORDS**
Magneto-elastic;
Conductor;
Dynamic behavior;
Magnetic field;
Structures.

**Abstract.** The main objective of this study is to investigate the vibration behavior of soft magnetoelastic plates mounted close to the rectangular conductors conducting current that can be efficiently applicable in structures. New relationships are derived for electromagnetic interaction forces with magnetoelastic plates using the general form of Maxwell's equations and Lorentz forces. Based on von-Kámán strain-displacement relations and Hamilton's principle, nonlinear differential equations are further derived for the plate through classical first-order shear deformation theory. This research numerically investigates how different parameters affect the resonance features of these plates by discretizing the nonlinear equations based on Galerkin method. The obtained results demonstrate that the intensity of the magnetic field and electric current profoundly affects the vibration behavior of the plates. Through these effects, loss of energy will happen in the plate which in turn results in a decrease in the oscillation amplitude over time.



## 1. Introduction

In recent decades, there has been a significant surge in the construction of structures using ferromagnetic and magnetoelastic materials in modern engineering [1–3]. These structures include beams, plates, and structures that can be modeled as beams or plates. Due to their wide variety of applications, these types of structures are usually placed in different environments and under different thermal, electrical, and magnetic loads [4–6]. Therefore, study of the mechanical behavior of these structures under a variety of loads significantly comes to the fore [7,8].

In order to analyze the dynamic response of the magnetoelastic plates, simplified assumptions are usually taken into account due to the interaction between the structure and magnetic field [9–11]. In [12], the linear mathematical equations was derived that governed the distribution of the magnetic forces and moments of a clamped plate located in a magnetic field. In another study [13], the impact of magnetic fields on the vibration behavior of plates was experimentally investigated. It was demonstrated that by excessing the intensity of the magnetic field applied to the magnetoelastic plate, the oscillation frequency of the plate would be reduced. Hasanyan et al. [14] studied the buckling and post-buckling of magnetoelastic plates

*. *Corresponding author.*
*E-mail address: afkar@standard.ac.ir (A. Afkar)*

doi: 10.24200/sci.2023.60532.6848

conducting electricity. Xue et al. [15] studied the nonlinear vibration of a magnetoelastic rectangular plate under the effect of magnetic field coupled with harmonic mechanical load. The bending deformation of a thin conductive plate exposed to the magnetic field was investigated in [16]. In [17], the nonlinear magnetoelastic dynamic equations of a shell as well as the electro-dynamic equations and expressions of the electro-magnetic forces were presented based on the Maxwell equations. Magnetic-structure coupling dynamic model of a ferromagnetic plate parallel moving in an air-gap magnetic field was investigated by Hu et al. [18]. The magnetic potential of the air-gap magnetic field was determined by the magnetic boundary conditions and separation of variables. Based on the magnetization force model and Lorentz force of ferromagnetic thin-walled structures as well as the electromagnetic constitutive relations and boundary conditions, a calculation model was established for the electromagnetic force of a soft ferromagnetic thin plate moving in an air-gap magnetic field.

Murodillayevich et al. [19] proposed a mathematical model and computational algorithm to simulate the vibration processes of thin magnetoelastic plates with complex shapes. Further, Hu and Xu [20] carried out an analysis of magnetoelastic coupling natural oscillations of annular plates in an induced non-uniform magnetic field. They derived the relevant expressions for the magnetic field, electromagnetic force, and torque acting on the plate based on the electromagnetic theory. They finally obtained an analytical second-approximation solution using multiple scales followed by the expressions for the first three nondimensional natural frequencies of the plate. Xu et al. [21] studied the magnetoelastic nonlinear free vibration of thin conductive annular plates under a nonuniform magnetic field generated by a long wire carrying current. Their results indicated that with an increase in the current, the natural frequency would be notably enhanced and then stabilized in the inner-clamped and out-clamped boundaries; however, it would be reduced and stabilized in the inner-simple and out-simple boundaries. Vlasov et al. [22] studied the nonlinear precession of the second-order magnetization in a magnetoelastic plate. Employing a model of potential, they developed a parametric portrait for magnetization and elastic displacement. An analytical study by Pourreza et al. [23] examined the buckling behavior of graphene nanosheets and their nonlinear vibrations in a magnetic field. Wang and Shih [24] investigated the vibration of a cracked rectangular plate subject to an in-plane force and a transverse magnetic field and supported at all its edges. In [25], Euler-Bernoulli approach was utilized to investigate the vibration of a ferromagnetic beam under a 3D magnetic field. In addition, the impact of the intensity and angle of the magnetic field on the system frequency was investigated. Kędzia et al. [26] numerically studied the vibration of polyethylene rectangular plates under the effect of magnetic forces. In one of the most recent studies in this field, Zhang et al. [27] used an analytical method to investigate the changes in the natural frequencies of Functionally Graded Porous (FGP) cylinders under the in-plane magnetic field. Hosseinian and Firouz-Abadi [28] conducted an investigation of the vibrations and stability of double current-carrying metal strips with a magnetic field. Firouz-Abadi and Hosseinian [29] studied the interaction between the vibrations and buckling of double current-carrying strips. In order to obtain four coupled equations of motion, they used Hamilton's principle to include the rotational and transverse deformations of the strip. They also employed Galerkin method to extract the mass and stiffness matrices and considered the eigenvalue problem to determine the stability of the system. In a real working area, Pourreza et al. [30] proposed an approach to determine the nonlinear vibration of the nanoplate carrying current located in the magnetic field. They concluded that the magnetic field decreased the nonlinear natural frequency of the nanoplate and increased the linear natural frequency.

Most magnetoelastic plates are exposed to magnetic fields created by conductors carrying current. Whenever a plate is placed near a conductor with current, additional magnetic stresses are generated in the plate, thus resulting in an alteration in their dynamic behavior and vibration characteristics. For this reason, it is important to study the effect of the conductors on the dynamics of magnetoelastic plates. However, few research has been done in this field, and the impact of the electric current and magnetic field on the nonlinear dynamic behavior of the conductive plates located in a magnetic field caused by conductors with the current has not been extensively investigated. As a result, new equations were derived for the electromagnetic tractions of magnetoelastic plates placed near conductors carrying electric current using a more realistic hypothesis. Based on Maxwell's electromagnetic theory and von Kámán strain-displacement relationships, new nonlinear motion equations were derived using the Hamilton's principle. Further, according to the Galerkin discretization and a numerical solution of the obtained nonlinear coupled equations, the impact of some factors on the dynamic performance of these plates were assessed.

## 2. Deriving motion equations

According to Figure 1, a homogeneous conductive plate made of soft magnetoelastic material with the length of $D$, width of $R$, and thickness of $H$ was exposed to the effect of magnetic field created by a conductor

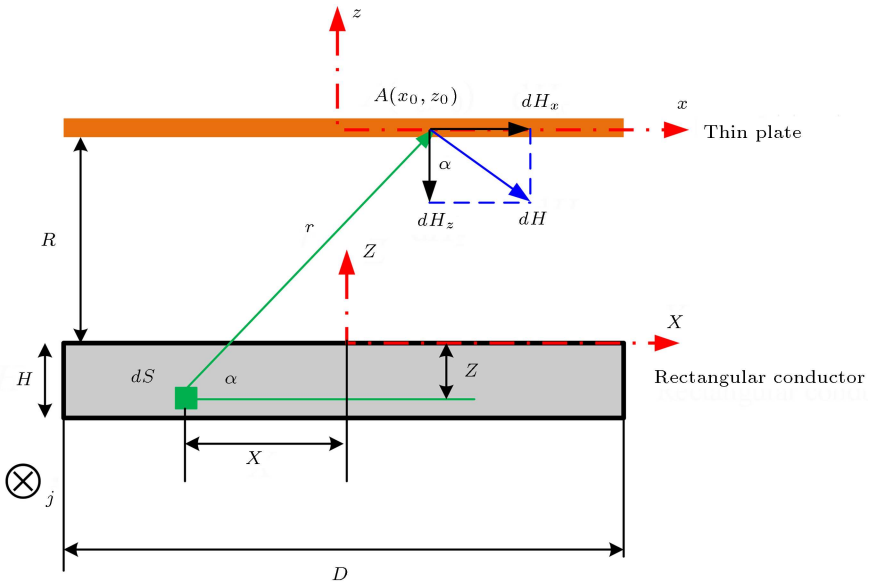


**Figure 1.** Geometry of the magnetoelastic plate affected by the magnetic field and rectangular conductor carrying electric current.

carrying electrical current and external mechanical load of $P$.

### *2.1. Magnetic fields equations*

Figure 1 illustrates the spatial distribution of the magnetic field determined in the proposed geometry where a magnetoelastic plate is placed under the effect of a rectangular conductor carrying electric current and external mechanical load.

Based on [31], the magnetic field **H** is genereted by the infinitely-long thin current-from distance $r$ in Gaussian approach, as shown below [32]:

$$|\mathbf{H}(x,y,z)| = \frac{1}{4\pi}\int \frac{|d\mathbf{j}\times\mathbf{r}|}{|\mathbf{r}|^2} \quad \left[\frac{\mathrm{A}}{\mathrm{m}}\right] = \frac{j}{2\pi r^2}, \tag{1}$$

where $j$ is the electrical current.

As shown in Figure 1 and according to Eq. (1), the magnetic field of elementary wire at any point $A(x,z)$ can be presented as Eq. (2) where the conductor cross-section is divided into infinite numbers of wires with section:

$$dH_x = \frac{j\sin\alpha}{2\pi r}dxdz,$$

$$dH_y = 0,$$

$$dH_z = -\frac{j\cos\alpha}{2\pi r}dxdz, \tag{2}$$

where $r = \sqrt{(x_0-X)^2+(z_0+Z)^2}$ is the slightest gap from the elementary wire to the position $A$, $\alpha$ angle among vector **r** and axis $X$, and:

$$\sin\alpha = \frac{z_0+Z}{\sqrt{(x_0-X)^2+(z_0+Z)^2}},$$

$$\cos\alpha = \frac{x_0+X}{\sqrt{(x_0-X)^2+(z_0+Z)^2}}. \tag{3}$$

The complete magnetic field in position $A(x_0,z_0)$ can be determined by a combination of expression of Eq. (2) across the conductor overlapped area:

$$H_x(x,z) = \int_0^H \int_{-D/2}^{D/2} dH_x(x_0,z_0)dXdZ$$

$$= \frac{j}{2\pi}\int_0^H \left[\int_0^{x+D/2} \frac{z_0+Z}{p^2+(z_0+Z)^2}dp - \int_0^{x-D/2} \frac{z_0+Z}{p^2+(z_0+Z)^2}dp\right]dZ, \tag{4}$$

$$H_z(x_0,z_0) = \int_0^H \int_{-D/2}^{D/2} dH_z(x_0,z_0)dXdZ$$

$$= \frac{j}{2\pi}\int_0^H \left[\int_0^{x+D/2} \frac{-p}{p^2+(z_0+Z)^2}dp + \int_0^{x-D/2} \frac{p}{p^2+(z+Z)^2}dp\right]dZ, \tag{5}$$

where $p$ represents the integrals of the $H_x$ and $H_z$, as follows:

$$H_x(x_0,z_0) = \frac{j}{2\pi}\int_0^H \int_0^p \frac{z_0+Z}{p^2+(z_0+Z)^2}dpdZ, \tag{6}$$

$$H_z(x_0,z_0) = \frac{j}{2\pi}\int_0^H \int_0^p \frac{-p}{p^2+(z_0+Z)^2}dpdZ, \tag{7}$$

which can be mentioned by the analytics functions:

$$H_x(x_0,z_0)=\frac{j}{4\pi}\left[p\ln\left(\frac{H^2+2z_0H}{p^2+z_0^2}\right)+2(z_0+H)\arctan\left(\frac{p}{z_0+H}\right)-2z\arctan\left(\frac{p}{z_0}\right)\right], \quad (8)$$

$$H_z(x_0,z_0)=\frac{j}{4\pi}\left[z_0\ln\left(1+\frac{p^2}{z_0^2}\right)-(z_0+H)\ln\left(\frac{p^2}{(z_0+H)^2}\right)-2p\arctan\left(\frac{z_0+H}{p}\right)+2p\arctan\left(\frac{z_0}{p}\right)\right]. \quad (9)$$

There is a magnetic constitutive equation of linear condition for the soft ferromagnetic materials [33]:

$$\mathbf{M}=\chi\mathbf{H} \quad \text{or} \quad \mathbf{B}=\mu_0\mu_r\mathbf{H}. \quad (10)$$

The force of body $\mathbf{f}=f_x\mathbf{i}+f_y\mathbf{j}+f_z\mathbf{k}$, body couple $\mathbf{c}=c_x\mathbf{i}+c_y\mathbf{j}+c_z\mathbf{k}$, and normal components $q_{Mech}\,(x,y,\pm h/2)$ of the external mechanical force on the faces of the plate are identified. Based on the thin plates theory [24], the equivalent lateral force can be obtained $q_z(x,y)$ as [33]:

$$q_z\,(x,y)=\int_{-h/2}^{h/2}f_z(x,y,z)dz+\frac{\partial}{\partial x}\int_{-h/2}^{h/2}c_y(x,y,z)dz-\frac{\partial}{\partial y}\int_{-h/2}^{h/2}c_x(x,y,z)dz+q_{Mech}\,(x,y,\pm h/2)\,. \quad (11)$$

Lorentz ponderomotive forces are representatives of the interaction between the mechanical and electromagnetic fields. Subsequently, the entire magnetic field in a position in a magnetic material is granted and then, the body force $\mathbf{f}$ and body couple $\mathbf{c}$ of Magnetic used on the body will be calculated as:

$$\mathbf{f}=\mathbf{M}.\nabla\mathbf{B}, \quad (12)$$

$$\mathbf{c}=\mathbf{M}\times\mathbf{B}. \quad (13)$$

By substituting Eq. (11) into Eqs. (12) and (13), we have:

$$\mathbf{f}=\frac{\mu_0\mu_r}{2}\nabla\left(\mathbf{H}^2\right). \quad (14)$$

### 2.2. Equations of motion

To obtain the equations governing the flexural vibration of the plate, the classical plate theory takes into account the von Kámán nonlinear strain-displacement relations. In this respect, the plate displacement fields are presented in terms of the middle plate deformations as:

$$u(x,y,z,t)=u_0(x,y,z,t)-z\phi_x(x,y,z,t),$$
$$v(x,y,z,t)=v_0(x,y,z,t)-z\phi_y(x,y,z,t),$$
$$w(x,y,z,t)=w_0(x,y,z,t). \quad (15)$$

In the above equation, $(u,v,w)$, $(u_0,v_0,w_0)$, and $(\phi_x,\phi_y)$ represent the displacement field components in the direction of $(x,y,z)$ axes, displacements of a point located in the middle plane of the plate, and rotation of the normal vectors around the $x$ and $y$ axes.

The strain-displacement relationships based on the first-order shear deformation plate approach are as follows:

$$\left\{\begin{array}{c}\varepsilon_x\\ \varepsilon_y\\ \gamma_{xy}\end{array}\right\}=\left\{\begin{array}{c}\varepsilon_x^{(0)}\\ \varepsilon_y^{(0)}\\ \gamma_{xy}^{(0)}\end{array}\right\}+z\left\{\begin{array}{c}\kappa_x\\ \kappa_y\\ \kappa_{xy}\end{array}\right\}, \quad (16)$$

where $\varepsilon_x^0,\varepsilon_y^0,\gamma_{xy}^0$ are the mid-plane strains that are define as:

$$\varepsilon_x^{(0)}=\frac{\partial v_0}{\partial y}+\frac{1}{2}\left(\frac{\partial w_0}{\partial y}\right)^2,$$
$$\varepsilon_y^{(0)}=\frac{\partial u_0}{\partial x}+\frac{1}{2}\left(\frac{\partial w_0}{\partial x}\right)^2,$$
$$\gamma_{xy}^{(0)}=\frac{1}{2}\left(\frac{\partial u_0}{\partial y}+\frac{\partial v_0}{\partial x}+\frac{\partial w_0}{\partial x}\frac{\partial w_0}{\partial y}\right),$$
$$\kappa_x=-\frac{\partial^2 w}{\partial x^2},\quad \kappa_y=-\frac{\partial^2 w}{\partial y^2},\quad \kappa_{xy}=-2\frac{\partial^2 w}{\partial x\partial y}. \quad (17)$$

Hamilton's principle is applied to derive the equations of motion. The Hamilton principle takes the following form:

$$\int_0^T(\delta K+\delta W-\delta U)dt=0, \quad (18)$$

where $\delta$, $K$, $W$, and $U$ represent the variation operator, kinetic energy, work done by the external forces, and strain potential energy, respectively, the values of which can be obtained as:

$$\delta K=\int_{\Omega_0}\int_{-\frac{h}{2}}^{\frac{h}{2}}\rho\left[\left(\dot{u}_0-z\frac{\partial\dot{w}_0}{\partial x}\right)\left(\delta\dot{u}_0-z\frac{\partial\delta\dot{w}_0}{\partial x}\right)+\left(\dot{v}_0-z\frac{\partial\dot{w}_0}{\partial y}\right)\left(\delta\dot{v}_0-z\frac{\partial\delta\dot{w}_0}{\partial y}\right)+\dot{w}_0\delta\dot{w}_0\right]dzdxdy, \quad (19)$$

$$\delta U = \int_{\Omega_0} \int_{-\frac{h}{2}}^{\frac{h}{2}} (\sigma_x \delta\varepsilon_x + \sigma_y \delta\varepsilon_y + 2\sigma_{xy}\delta\varepsilon_{xy}) dz dx dy$$

$$= \int_{\Omega_0} \left\{ \int_{-\frac{h}{2}}^{\frac{h}{2}} \left[ \sigma_x \left( \delta\varepsilon_x^{(0)} + z\delta\varepsilon_x^{(1)} \right) + \sigma_y \left( \delta\varepsilon_y^{(0)} + z\delta\varepsilon_y^{(1)} \right) + \sigma_{xy} \left( \delta\gamma_{xy}^{(0)} + z\delta\gamma_{xy}^{(1)} \right) \right] dz \right\} dx dy, \quad (20)$$

$$\delta V = \int_{\Omega_0} p(x,t)\delta w_0 \, dx dy, \quad (21)$$

where $p(x,t)$ indicates the external forces applied to the plate.

By defining the resultant force and moment, we have:

$$(N_{xx}, N_{yy}, N_{xy}) = \int_{-\frac{h}{2}}^{\frac{h}{2}} (\sigma_{xx}, \sigma_{yy}, \sigma_{xy}) \, dz,$$

$$(M_{xx}, M_{yy}, M_{xy}) = \int_{-\frac{h}{2}}^{\frac{h}{2}} (\sigma_{xx}, \sigma_{yy}, \sigma_{xy}) \, z dz,$$

$$(I_0, I_1, I_2) = \rho \int_{-\frac{h}{2}}^{\frac{h}{2}} \left(1, , z, z^2\right) dz. \quad (22)$$

By substituting Eqs. (18)–(20) into Eq. (17) and through the unity the coefficients of $\delta u_0$, $\delta v_0$, and $\delta w_0$ on the two sides of the relation, we can obtain the governing equations of motion as:

$$\delta u_0 : \quad \frac{\partial N_{xx}}{\partial x} + \frac{\partial N_{xy}}{\partial y} + f_x = I_0 \frac{\partial^2 u_0}{\partial t^2} - I_1 \frac{\partial^2}{\partial t^2} \left( \frac{\partial w_0}{\partial x} \right),$$

$$\delta v_0 : \quad \frac{\partial N_{xy}}{\partial x} + \frac{\partial N_{yy}}{\partial y} + f_y = I_0 \frac{\partial^2 v_0}{\partial t^2} - I_1 \frac{\partial^2}{\partial t^2} \left( \frac{\partial w_0}{\partial y} \right),$$

$$\delta w_0 : \quad \frac{\partial^2 M_{xx}}{\partial x^2} + 2\frac{\partial^2 M_{xy}}{\partial x \partial y} + \frac{\partial^2 M_{yy}}{\partial y^2} + \mathbb{N}(w_0) + q_z = I_0 \frac{\partial^2 w_0}{\partial t^2} - I_2 \frac{\partial^2}{\partial t^2} \left( \frac{\partial^2 w_0}{\partial x^2} + \frac{\partial^2 w_0}{\partial y^2} \right) + I_1 \frac{\partial^2}{\partial t^2} \left( \frac{\partial u_0}{\partial x} + \frac{\partial v_0}{\partial y} \right). \quad (23)$$

It should be noted that these force components are created in the plate by the magnetic field and electric current, and these terms are not incorporated in the conducted studies by other researchers in this field.

For uniform isotropic plate, the outcomes of the forces and bending moments are obtained as follows:

$$\begin{Bmatrix} N_{xx} \\ N_{yy} \\ N_{xy} \end{Bmatrix} = \frac{Eh}{1-v^2} \begin{bmatrix} 1 & v & 0 \\ v & 1 & 0 \\ 0 & 0 & 0 \end{bmatrix} \begin{Bmatrix} \varepsilon_x^0 \\ \varepsilon_y^0 \\ \gamma_{xy}^0 \end{Bmatrix},$$

$$\begin{Bmatrix} M_{xx} \\ M_{yy} \\ M_{xy} \end{Bmatrix} = \frac{h^2}{12} A \begin{bmatrix} 1 & v & 0 \\ v & 1 & 0 \\ 0 & 0 & 0 \end{bmatrix} \begin{Bmatrix} \varepsilon_x^{(1)} \\ \varepsilon_y^{(1)} \\ \gamma_{xy}^{(1)} \end{Bmatrix}. \quad (24)$$

Lastly, by determining the axial and shear forces as well as the bending moments of Eq. (24) based on the assumptions of the beam-plate approach and also ignoring the longitudinal inertia along the $x$ and $y$ axes, we can derive the equation governing the flexural vibration behavior of the magnetoelastic plate placed near the current caring conductor using Eq. (23) as:

$$A_{66} \left( \frac{\partial^2 v_0}{\partial x^2} + \frac{\partial^2 u_0}{\partial x \partial y} + \frac{\partial w_0}{\partial x}\frac{\partial^2 w_0}{\partial x \partial y} + \frac{\partial w_0}{\partial y}\frac{\partial^2 w_0}{\partial x^2} \right) + A_{12} \left( \frac{\partial w_0}{\partial x}\frac{\partial^2 w_0}{\partial x \partial y} + \frac{\partial^2 u_0}{\partial x \partial y} \right) + A_{22} \left( \frac{\partial w_0}{\partial y}\frac{\partial^2 w_0}{\partial y^2} + \frac{\partial^2 v_0}{\partial y^2} \right) + f_x = -I_1 \frac{\partial^2}{\partial t^2} \left( \frac{\partial w_0}{\partial x} \right), \quad (25)$$

$$A_{11} \left( \frac{\partial w_0}{\partial x}\frac{\partial^2 w_0}{\partial x^2} + \frac{\partial^2 u_0}{\partial x^2} \right) + A_{12} \left( \frac{\partial w_0}{\partial y}\frac{\partial^2 w_0}{\partial x \partial y} + \frac{\partial^2 v_0}{\partial x \partial y} \right) + A_{66} \left( \frac{\partial^2 v_0}{\partial x \partial y} + \frac{\partial^2 u_0}{\partial y^2} + \frac{\partial w_0}{\partial x}\frac{\partial^2 w_0}{\partial y^2} + \frac{\partial w_0}{\partial y}\frac{\partial^2 w_0}{\partial x \partial y} \right) + f_y = -I_1 \frac{\partial^2}{\partial t^2} \left( \frac{\partial w_0}{\partial y} \right), \quad (26)$$

$$-D_{11}\frac{\partial^4 w_0}{\partial x^4} - 2(D_{12} + 2D_{66})\frac{\partial^4 w_0}{\partial x^2 \partial y^2} - D_{22}\frac{\partial^4 w_0}{\partial y^4} + N(w_0) = I_0 \frac{\partial^2 w_0}{\partial t^2} + I_1 \frac{\partial^2}{\partial t^2} \left( \frac{\partial u_0}{\partial x} + \frac{\partial v_0}{\partial y} \right) - I_2 \frac{\partial^2}{\partial t^2} \left( \frac{\partial^2 w_0}{\partial x^2} + \frac{\partial^2 w_0}{\partial y^2} \right) + q_z(x,t). \quad (27)$$

### 2.3. Solution method

For the vibrations of thin magnetoelastic plates, the Bubnov-Galerkin variation method was employed to

solve the governing Eqs. (25)–(27). The Bubnov-Galerkin method is the most widely used weighted average method [34–36]. This problem can be solved through the following steps:

1. Creation of a sequence of coordinate functions that satisfy the specified boundary conditions;
2. Substitution of the coordinate functions in the governing equations and integrating the result over the whole plate area;
3. Discretization versus spatial variables, i.e., construction of discrete equations;
4. Numerical solution of the discrete equations and determination of unknown components of solution structures;
5. Determination of unknown functions. Of note, the tangential displacement and normal displacement of the middle plate are also determined in this step.

In the first step, the constructive method of normal mode shapes is used to construct a sequence of coordinate functions that meet the boundary conditions given the complex plate. Note that the vibration mode shapes build a sequence of coordinate functions in the form of the structure of solutions satisfying the boundary conditions at almost any complex configuration contour of plates in the plan. In accordance with the simple supported boundary conditions around the plate, the following coordinate functions can be expressed as:

$$u_0(x,y,t)=\sum_{n=1}^{N}\sum_{m=1}^{M}U_{mn}(t)\sin\frac{2m\pi x}{a}\sin\frac{n\pi y}{b},$$

$$v_0(x,y,t)=\sum_{n=1}^{N}\sum_{m=1}^{M}V_{mn}(t)\sin\frac{m\pi x}{a}\sin\frac{2n\pi y}{b},$$

$$w_0(x,y,t)=\sum_{n=1}^{N}\sum_{m=1}^{M}W_{mn}(t)\sin\frac{m\pi x}{a}\sin\frac{n\pi y}{b}, \quad (28)$$

where $m$ and $n$ are both positive integers denoting different vibrations modes of the magnetoelastic plate. Here, $U_{mn}(t)$, $V_{mn}(t)$, and $W_{mn}(t)$ are the general coordinates. By substituting the hypothetical solution Eqs. (28) into Eqs. (25)-(27) and using the Galerkin approach, the equations of motion are discretized as nonlinear coupled Ordinary Differential Equations (ODEs) based on which the unknown functions of standard coordinates can be determined.

For $N=1$ and $M=1$, through the Galerkin approach, both $U(t)$ and $V(t)$ functions will be obtained in terms of $W(t)$ from Eqs. (25) and (26). By substituting these functions into Eq. (27), the nonlinear differential equation governing time section of the megnetoelastic plate flexural deflection, which is a second-order differential equation, can be derived as:

$$\frac{d^2W(t)}{dt^2}+\alpha_1W(t)+\alpha_2W^2(t)+\alpha_3W^3(t)+\alpha_4\frac{dW(t)}{dt}=\lambda\sin(\Omega t), \quad (29)$$

where the $\alpha_i$ coefficients are the constant components of the stiffness matrices and geometric derivatives of the plate. The values of these constants for $n=m=1$ are obtained as:

$$\alpha_1=-\frac{\pi^2}{I_0a^4b^4}\Big(\pi^2Da^4+b^4\pi^2D+R_9a^4b^2-I_2b^4a^2+R_7b^4a^2+2\pi^2D\nu a^2b^2-I_2a^4b^2\Big),$$

$$\alpha_2=\frac{16}{9I_0\left(256\nu^2-81\pi^4\right)a^4b^4}\Big(-162R_4\pi^4b^4+81R_1b^2\pi^4-144R_1\pi^2a^2\nu^2+512\nu^2R_4b^2\Big),$$

$$\alpha_3=\frac{16}{9I_0\left(256\nu^2-81\pi^4\right)a^4b^4}\Big(-162R_4\pi^4b^4+81R_1b^2\pi^4-144R_1\pi^2a^2\nu^2+512\nu^2R_4b^2\Big),$$

$$\alpha_4=\frac{-1}{32I_0\left(256\nu^2-81\pi^4\right)\pi^2a^4b^4}\Big\{729\nu\pi^4b^4+81\pi^4b^2a^2-2304\pi^2b^4+1152\nu\left(1+\nu\right)\pi^2b^2a^2-2304\pi^2\nu\left(a_4+\nu^2b^4\right)-2048\nu^2b^4+4096\nu a^2b^2+3840\nu^2a^2b^2-2048\nu^3a^4\Big\}. \quad (30)$$

Once Eq. (29) is solved using the fourth-order Runge-Kutta method and consequently, the associated vibration mode and phase plane can be obtained. The time step used in the computation is $t=0.0001$. In each case, the plate is assumed to be initially at rest, that is, roots at $\dot{w}(t)=0$. The following section evaluates the impact of different parameters on the dynamic behavior of magnetoelastic plates under magnetic fields using this numerical solution.

## 3. Results and discussion

The purpose of this study is to evaluate the effects of the intensity of the magnetic field, electrical current in the conductor, and imposed mechanical force on the dynamic and vibration behavior of the plate. In the current research, aluminum is assumed to be the material of the magnetoelastic plate. The geometric and mechanical characteristics of this plate are shown in Table 1. An error of $1\times10^{-6}$ is considered in all numerical results.

**Table 1.** Geometric and mechanical characteristics of magnetoelastic plate.

| Parameter | Values |
|---|---|
| Density, $\rho$ (kg/m$^3$) | 2450 |
| Elastic modulus, $E$ (GPa) | 72 |
| Poisson's ratio, $\nu$ | 0.26 |
| Thickness, $h$ (mm) | 1.70 |
| Length, $L$ (mm) | 150 |
| Magnetic permeability, $\mu$ $(H/m)$ | $3 - 6 \times 10^{-5}$ |
| Conductivity, $\sigma$ | $1.3 \times 10^6$ |
| Susceptibility of the soft ferromagnetic medium, $\chi_m$ | 6 |

**Table 2.** linear and nonlinear resonance frequency of the simply supported magnetoelastic plate with the intensity of the electrical current.

| | $R/H = 10$ | | | $R/H = 2$ | | |
|---|---|---|---|---|---|---|
| $J$ | $\Omega_L$ | $\Omega_N$ | $\Omega_N/\Omega_L$ | $\Omega_L$ | $\Omega_N$ | $\Omega_N/\Omega_L$ |
| 0 | 5.71 | 5.45 | 0.95 | 5.32 | 3.42 | 0.64 |
| 5 | 7.37 | 5.34 | 0.72 | 6.41 | 2.61 | 0.41 |
| 10 | 8.86 | 5.28 | 0.60 | 7.57 | 2.04 | 0.27 |
| 15 | 10.10 | 3.72 | 0.37 | 8.13 | 1.56 | 0.19 |
| 20 | 12.48 | 1.09 | 0.09 | 10.96 | 1.03 | 0.09 |

### *3.1. Free vibrations*

This section examines the vibration characteristics of the plate including the response of free vibrations and natural frequency. In order to determine the free vibration response of a system, the external mechanical excitation force in Eq. (29) is assumed to be zero. Initially, we investigated the effect of electric current intensity on the dynamic behavior of the central point of the plate in the absence of external mechanical forces. In Figure 2, the plate response is illustrated for different values of the electric current and $R/H = 10$ without mechanical forces. As demonstrated in Figure 2(a), the system response oscillates with a constant amplitude in the absence of the electric current. The electric current dissipates energy as the current density of the conductor increases, thus resulting in a reduction in the oscillation amplitude. Given that energy consumption in the plate increases upon increasing the current intensity, buckling does not occur. In addition, the electric current causes permanent deflection in the plate and as the intensity of electric current increases, the steady state deflection of the plate increases even more. According to the results from Figure 2(b) and (c), the steady state deflections of the plate for the current density $2 \times 10^2$ A/m$^2$ and $4 \times 10^2$ A/m$^2$ are equal to 0.44 mm and 0.8 mm, respectively. The steady state deflection increases up to 82% when the current density is doubled. Therefore, increasing the electric current applied to the conductor decreases its equivalent stiffness, thus resulting in an increase in the system oscillation amplitude.

Furthermore, according to the spectrum curve, the electrical current has a significant effect on the frequency of oscillations in the system. Increasing the current intensity results in a decrease in the natural frequency. For the current density of $2 \times 10^2$ A/m$^2$ and $4 \times 10^2$ A/m$^2$, the natural frequencies are obtained as 4.26 Hz and 2.31 Hz, respectively. Hence, as the current increases up to 100%, the natural frequency decreases by approximately 46% due to the effect of the electric current on the equivalent rigidity of the structure. As observed in Figure 2, with the application of the electric current, the rigidity of the structure is reduced, thus resulting in a reduction in the normal frequency of the system as well as the sheet durability.

Table 2 shows the linear and nonlinear resonance frequency of the simply supported magnetoelastic plate as a function of the intensity of the electrical current. According to this table, the linear natural frequency increases upon increasing the electrical current intensity but the nonlinear frequency decreases substantially. It is believed that this behavior arises from the fact that as the current intensity increases, the effect of geometrical nonlinear terms becomes more intensified, thus resulting in a dramatic decrease in the ratio of nonlinear frequency to the linear frequency. These results suggest that the coefficient of nonlinear sentences increases as the intensity of the electrical current

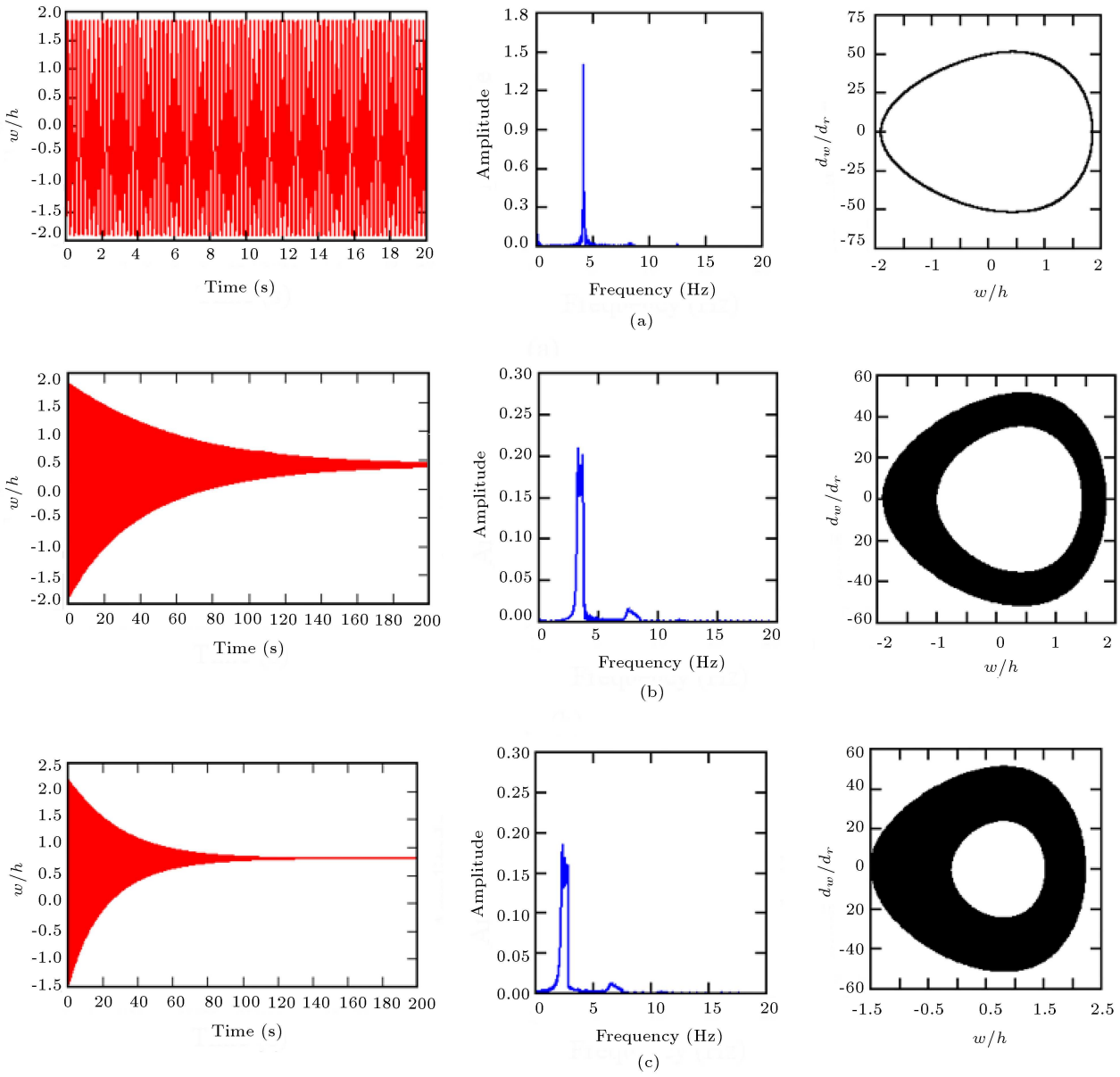


**Figure 2.** Time response, phase portraits, and spectrum of the magnetoelastic plate for different values of the electric current intensity of the conductor: (a) $J = 0$, (b) $J = 2 \times 10^2$ A/m$^2$, and (c) $J = 4 \times 10^2$ A/m$^2$.

increases; therefore, in order to achieve accurate and realistic geometric irritation results at larger values, the intensity of the electrical current must be taken into consideration.

Figure 3 shows the plate time trace for three different values of $R/H$ and current intensity of $0.4 \times 10^3$ A/m$^2$. The results show that for high value of $R/H$, the system response will be oscillating. In addition, the magnetic field causes nonlinear damping in the Lorentz force (Eq. (11)) which depends on the intensity of the magnetic field, electric current, and $R/H$. As the $R/H$ intensifies, the magnetic damping increases, hence increased energy dissipation. This causes the oscillation amplitude to move towards the steady state, as depicted in Figure 3. According to this figure, for the $R/H$ values of 1 and 10, the steady state deflections of the system are 2.4 mm and 9.2 mm, respectively, indicating the significant impact of the magnetic field and distance between the plat and conductor on the deformation of the magnetoelastic plates. Table 3 demonstrates the plate steady state deflection for different values of $R/H$ and electric current intensity. According to the observations, upon increasing the $R/H$ value and electric current, the steady-state deflection decreases. It should be noted that the $R/H$ effect on the plate steady state deflection is much greater than that of the electric current. Upon increasing the $R/H$ and electric current up to 10

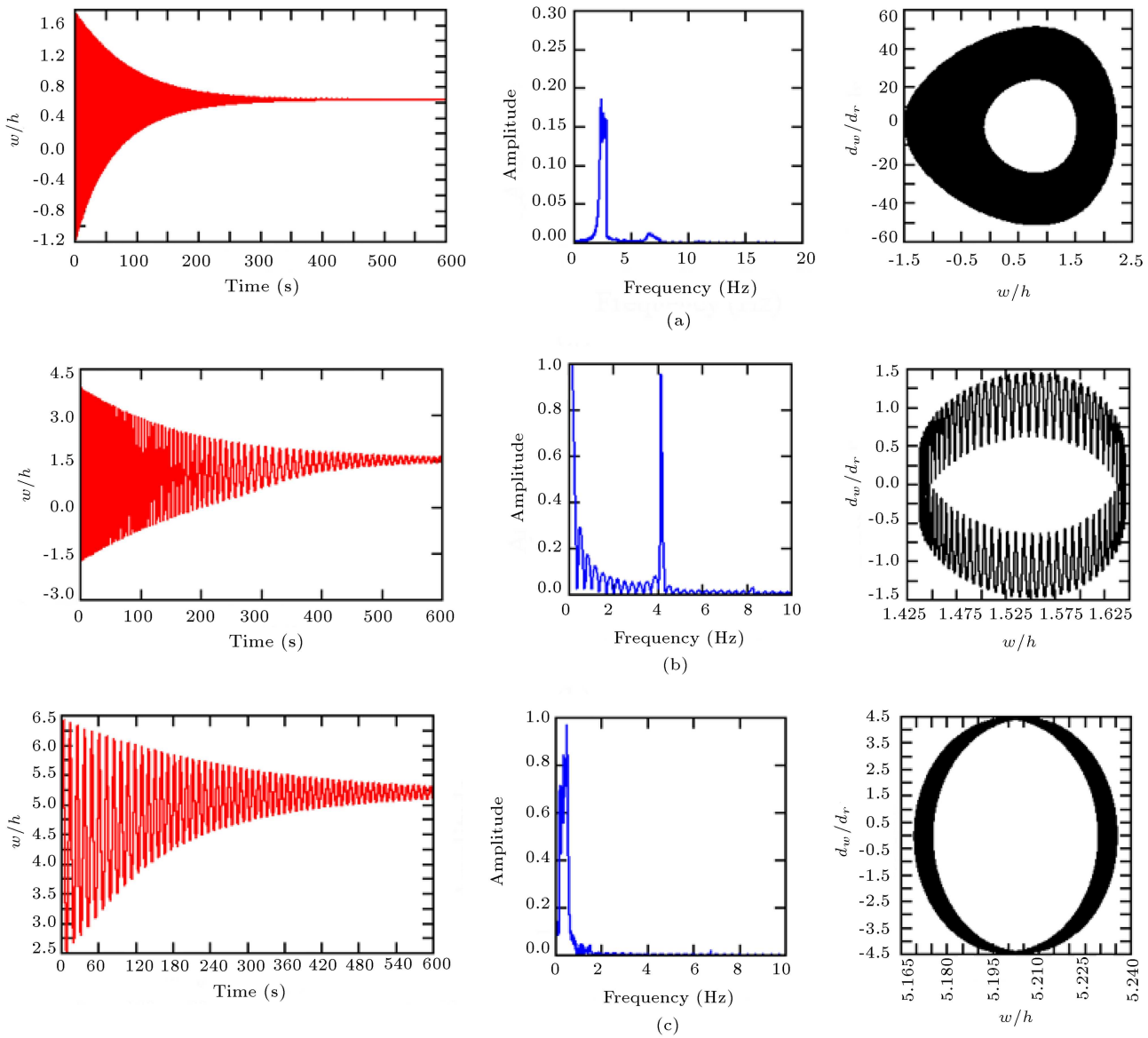


**Figure 3.** Time traces of the conductive plate under the effect of different field intensity values: (a) $R/H = 20$, (b) $R/H = 10$, and (c) $R/H = 1$.

**Table 3.** Steady-state deflection of the plate for different values of $R/H$ and electric current intensity.

| $R/H$ | | | | | | |
|---|---|---|---|---|---|---|
| **1** | **2** | **5** | **10** | **15** | **20** | $\boldsymbol{J}$ **(A/m$^2$)** |
| 5.24 | 4.38 | 3.88 | 1.58 | 1.14 | 0.64 | 20 |
| 8.45 | 7.05 | 5.01 | 2.05 | 1.35 | 0.68 | 50 |
| 9.69 | 8.05 | 5.64 | 2.21 | 1.44 | 0.70 | 100 |
| 10.09 | 8.36 | 5.83 | 2.27 | 1.47 | 0.78 | 150 |
| 10.55 | 8.71 | 6.04 | 2.32 | 1.49 | 0.85 | 200 |
| 11.21 | 9.12 | 6.27 | 2.37 | 1.52 | 0.93 | 400 |
| 11.52 | 9.45 | 6.47 | 2.43 | 1.55 | 1.21 | 1000 |

times, the maximum steady state deflection of the plate changes by about 350% and 3.8%, respectively. OF note, a decrease in the oscillation amplitude can be observed by reducing plate distance from the conductor and intensifying the electrical current intensity.

Since oscillation frequency in nonlinear systems is a function of amplitude, changing the amplitude of response oscillation causes variations in the frequency of the system. As the results show, applying electric current reduces the amplitude of the conductive plate oscillations over time by damping the Lorentz force. As a result, the frequency of the oscillations will also change with time, as clearly shown in Figure 4. In this figure, the response wavelet of the conductive plate proved to be affected by the magnetic field for the $R/H$ values 20, 10, and 1. The results show that in the large value of $R/H$, the first two frequencies of the system are about 5 Hz and 20 Hz (Figure 4(a)). Upon applying the magnetic field, the frequency of nonlinear oscillations will increase. For $R/H = 10$, the first two frequencies of the system at the initial moment are about 25 Hz and 65 Hz (Figure 4(b)). As observed in Figure 4(c), for $R/H = 1$, the first two frequencies of the system at the initial moment are about 38 Hz and 92 Hz. The amplitude of the oscillations decreases over time in the presence of the magnetic field, and the frequency of oscillations in nonlinear systems is a function of the amplitude; hence, it can be concluded that the nonlinear frequency decreases with time. These changes become more intense upon increasing the $R/H$.

### *3.2. Forced vibration*

Nonlinear behavior in the system triggers other different behaviors in the system depending on the boundary conditions and excitation force parameters. Figures 5–7 indicate the time traces, phase portraits, and Poincaré graphs of the conductive plate under the effect of mechanical force for different values of excitation frequency. It should be noted that these curves are plotted for $R/H = 5$. According to the observations, different nonlinear dynamic behaviors appear in the system according to the frequency of the external excitation force. According to Figure 5, at the excitation frequency of 10 Hz, the system exhibits a harmonic behavior, and the Poincaré map shows only one point. As the excitation frequency increases, the system behavior will change, and quasi-periodic motion will occur at the excitation frequency of 12.3 Hz, as shown in Figure 6. The chaotic motion at the excitation frequency of 14.2 Hz is demonstrated in Figure 7 where the Poincaré map expresses self-similarity.

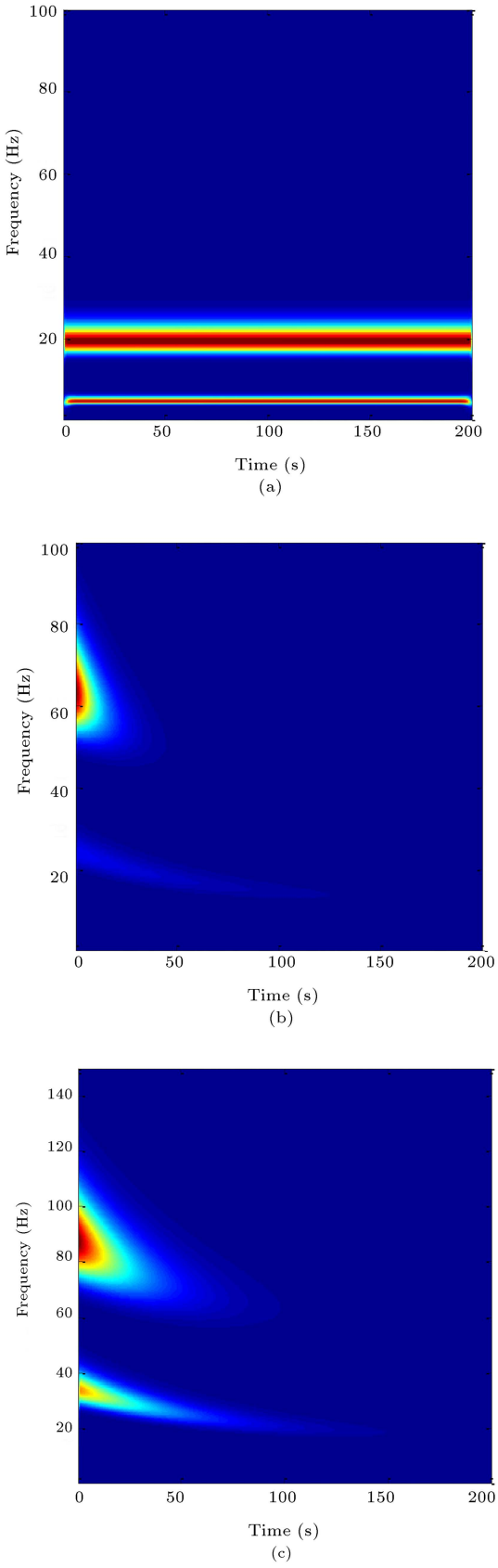


**Figure 4.** Wavelet transform of the time response for different values of the $R/H$: (a) $R/H = 20$, (b) $R/H = 10$, and (c) $R/H = 1$.

## 4. Conclusion

A nonlinear differential equation was developed in

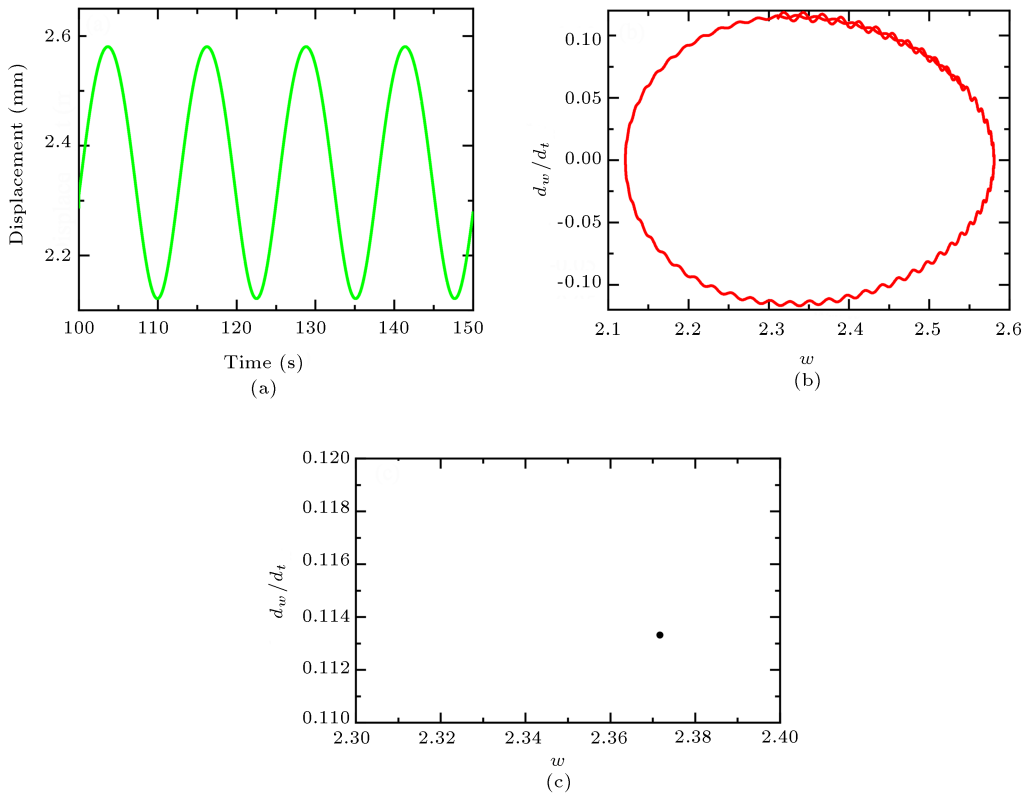


**Figure 5.** Harmonic motion of the system: (a) time trace, (b) phase portrait, and (c) Poincaré map.

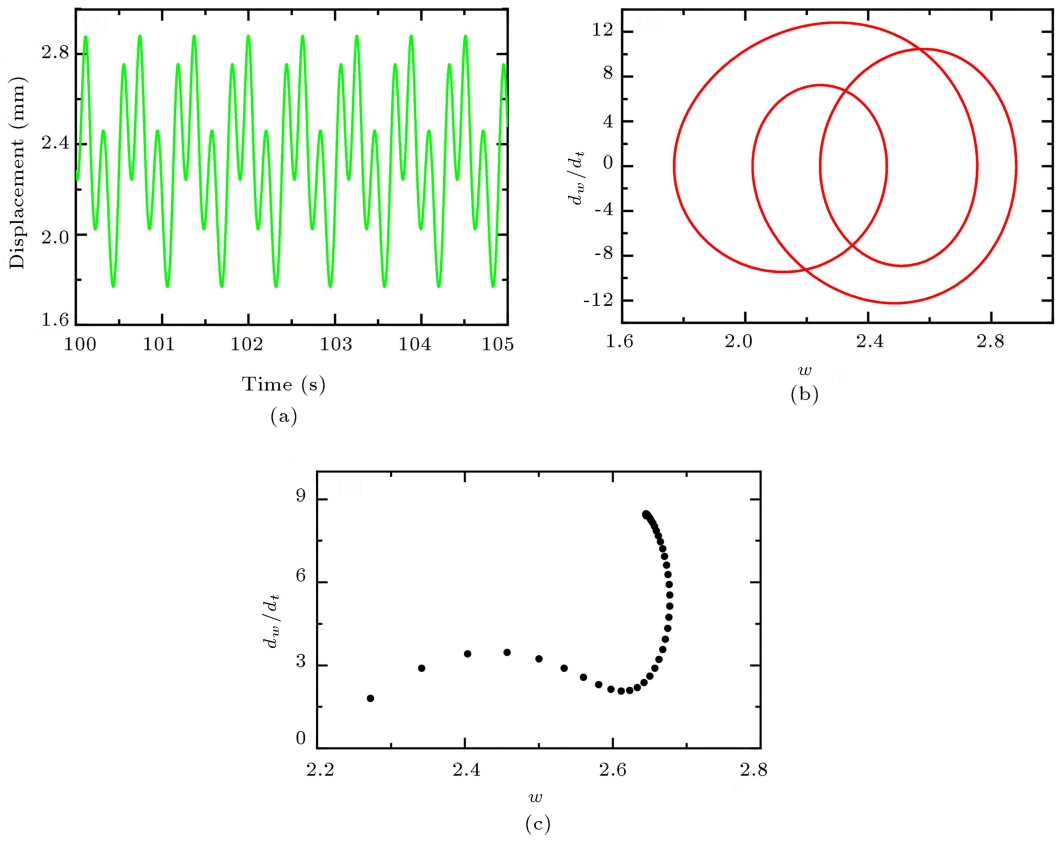


**Figure 6.** Quasi-periodic motion of the system: (a) time trace, (b) phase portrait, and (c) Poincaré map.

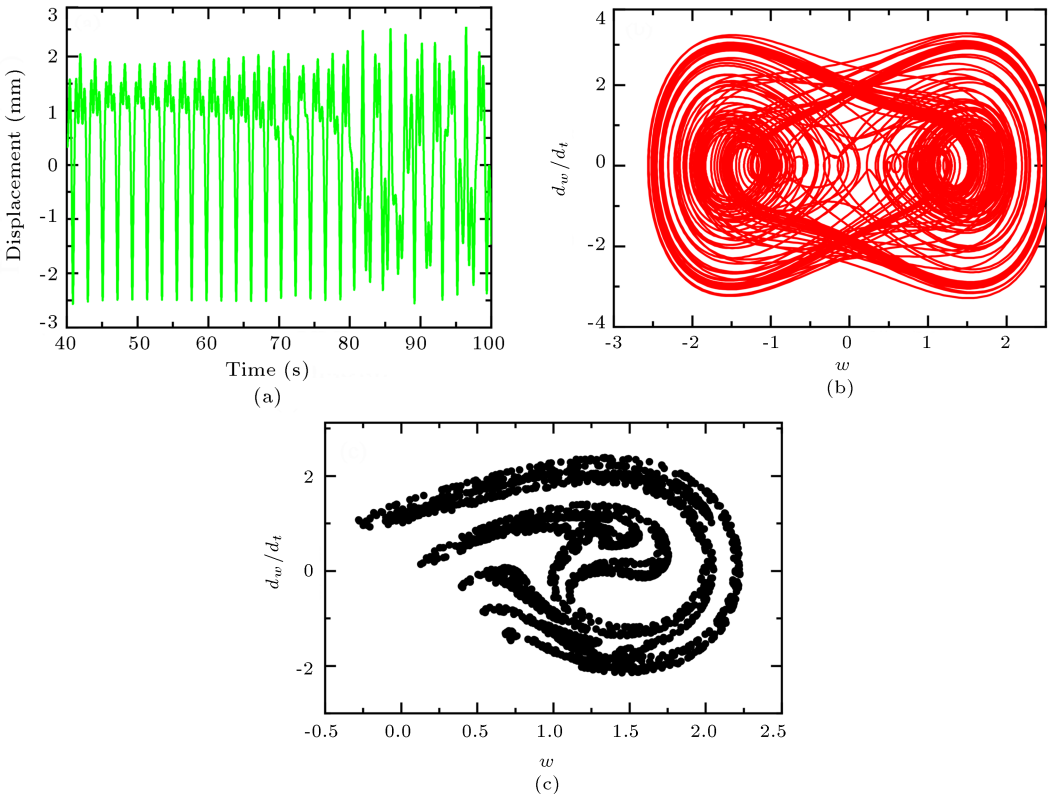


**Figure 7.** Chaotic motion of the system: (a) time trace, (b) phase portrait, and (c) Poincaré map.

this research that could govern the flexural dynamic behavior of the magnetoelastic plates located near the conductor plates with electrical current under the effect of electric currents and external mechanical forces. Followed by discretization of the motion equations therough the Galerkin method, the effects of different parameters on the vibration parameters of the system were numerically studied by solving the equations. The nonlinear performance of the system was then investigated using time traces, phase portraits, Poincaré maps, and instantaneous nonlinear frequencies for different values of system parameters. A summary of the conclusions are given below:

- Intensification of the electric currents and external mechanical forces in the equations of motion resulted in novel components with influential effects on the vibration characteristics of the magnetoelastic plates;
- As a result of the exposure of the conductive plates to the magnetic field and electrical current, damping occurred in the system which in turn reduced the amplitude of oscillations;
- A decrease in the oscillation amplitude was observed while decreasing the plate distance from the conductor and increasing the electrical current intensity;
- The system showed different types of behavior including harmonic, quasi-periodic, and chaotic motions, depending on the parameters of the excitation force.

## Nomenclature

### *Symbols*

| | |
|---|---|
| $A$ | Position |
| $abs$ | Absorber |
| $Lm$ | Susceptibility of the soft ferromagnetic medium |
| $C_p$ | Specific heat (J/kg.K) |
| $U_0$ | Magnetic permeability |
| $D$ | Diameter (m) |
| $e$ | Specific exergy (kJ/kg), evaporator |
| $H$ | Magnetic field |
| $I_b$ | Beam irradiance (W.m$^{-3}$) |
| $K$ | Kinetic energy |
| $\dot{m}$ | Mass flow rate (kg/s) |
| $M$ | Molecular mass (kg/kmol) |
| $n$ | Number of solar collectors, day number |
| $P$ | Pressure (bar), pump |
| $q$ | External mechanical force |
| $U$ | Strain potential energy |
| $w_a$ | Aperture width (m) |

| | |
|---|---|
| $W$ | Work (kJ) |
| $\dot{W}$ | Power (kW) |
| $Y_d$ | Exergy destruction ratio (%) |
| $R/H$ | Dimensionless distance |
| $L$ | Length plate |
| $h$ | Thickness of plate |
| OMC | Operation and Maintenance Cost |

***Greek symbols***

| | |
|---|---|
| $\eta$ | Efficiency |
| $\alpha$ | Angle |
| $\varepsilon$ | Strains |
| $\delta$ | Variation operator |
| $\rho$ | Density of mass |
| $v$ | Young modulus |
| $\sigma$ | Conductivity |

***Subscripts***

| | |
|---|---|
| $D$ | Destruction |
| $Aux$ | Auxiliary heater |
| $i$ | Inlet |
| $e$ | Exit |
| $s$ | Isentropic |
| $f$ | Saturated liquid |
| $ref$ | Reference |
| CV | Control Volume |
| $sat$ | Saturated |
| $t$ | Time |
| $e.v$ | Expansion valve |

***Abbreviations***

| | |
|---|---|
| EUF | Energy Utilization Factor |
| LHV | Lower Heating Value |

## References


1. She, S., Chen, Y., He, Y., et al. "Optimal design of remote field eddy current testing probe for ferromagnetic pipeline inspection", *Measurement*, **168**, pp. 33–45 (2021).
2. Yuan, F., Yu, Y., Wang, W., et al. "Pulsed eddy current array design and electromagnetic imaging for defects detection in metallic materials", *Nondestructive Testing and Evaluation*, **56**, pp. 1–19 (2021).
3. Kassanos, P., Rosa, B.G., Keshavarz, M., et al. "From wearables to implantables-clinical drive and technical challenges", *Wearable Sensors*, **8**, pp. 29–84 (2021).
4. Madina, B. and Gumilyov, L.N. "Determination of the most effective location of environmental hardenings in concrete cooling tower under far-source seismic using linear spectral dynamic analysis results", *Journal of Research in Science, Engineering and Technology*, **29**(1), pp. 22–24 (2020).
5. Assadi, A., Najaf, H., and Nazemizadeh, M. "Size-dependent vibration of single-crystalline rectangular nanoplates with cubic anisotropy considering surface stress and nonlocal elasticity effects", *Thin-Walled Structures*, **170**, 108518 (2022).
6. Liang, X., Dong, C., Chen, H., et al. "A review of thin-film magnetoelastic materials for magnetoelectric applications", *Sensors*, **20**(5), 1532 (2020).
7. Minaev, A.J. and Korovkin, J.V. "Vibration studies of a magnetoelastic material", in *IOP Conference Series: Materials Science and Engineering. IOP Publishing*, **91** (2020).
8. Ren, L., Yu, K., and Tan, Y. "Applications and advances of magnetoelastic sensors in biomedical engineering: A review", *Materials*, **12**(7), 1135 (2019).
9. Xu, X., Han, Q., and Chu, F. "Nonlinear vibration of a rotating cantilever beam in a surrounding magnetic field", *International Journal of Non-Linear Mechanics*, **95**, pp. 59–72 (2017).
10. Youhe, Z. and Xiaojing, Z. "A theoretical model of magnetoelastic bucking for soft ferromagnetic thin plates", *Acta Mechanica Sinica*, **12**(3), pp. 213–224 (1996).
11. Wu, B. and Destrade, M. "Wrinkling of soft magneto-active plates", *International Journal of Solids and Structures*, **208**, pp. 13–30 (2021).
12. Molaei, S., Ghorbani, N., Dashtiahangar, F., et al. "FDCNet: Presentation of the fuzzy CNN and fractal feature extraction for detection and classification of tumors", *Computational Intelligence and Neuroscience*, **2022**, 7543429 (2022).
13. Karami, S. and Saeedi Dehaghani, A. "Sensitivity analysis of electromagnetic stimulation of oil wells using simulation technique and Box-Behnken design", *Scientia Iranica*, **29**(3), pp. 1377–1390 (2022).
14. Hasanyan, D.J., Librescu, L., and Ambur, D.R. "Buckling and postbuckling of magnetoelastic flat plates carrying an electric current", *International Journal of Solids and Structures*, **43**(16), pp. 4971–4996 (2006).
15. Xue, C., Pan, E., Han, Q., et al. "Non-linear principal resonance of an orthotropic and magnetoelastic rectangular plate", *International Journal of Non-Linear Mechanics*, **46**(5), pp. 703–710 (2011).
16. Zheng, X., Zhang, J., and Zhou, Y. "Dynamic stability of a cantilever conductive plate in transverse impulsive magnetic field", *International Journal of Solids and Structures*, **42**(8), pp. 2417–2430 (2005).
17. Li, J. "Magneto-elastic combination resonances analysis of current-conducting thin plate", *Applied Mathematics and Mechanics*, **29**(8), pp. 1053–1066 (2008).
18. Hu, Y., Cao, T., and Xie, M. "Magnetic-structure coupling dynamic model of a ferromagnetic plate parallel moving in air-gap magnetic field", *Acta Mechanica Sinica*, **38**(10), pp. 1–11 (2022).

19. Murodillayevich, N.F., Sharibayevich, A.B., and Artikbayevich, A.M. "Mathematical model and computational algorithm of vibration processes of thin magnetoelastic plates with complex form", *International Conference on Information Science and Communications Technologies (ICISCT)*. IEEE (2021).

20. Hu, Y. and Xu, H. "Nonaxisymmetric magnetoelastic coupling natural vibration analysis of annular plates in an induced nonuniform magnetic field", *Nonlinear Dynamics*, **7**, pp. 1–31 (2022).

21. Xu, H., Hu, Y., and Hao, Y. "Magnetoelastic nonlinear free vibration of an annular plate under a nonuniform magnetic field of the long straight current-carrying wire. ZAMM", *Journal of Applied Mathematics and Mechanics*, **102**(6), 202000299 (2022).

22. Vlasov, V.S., Kirushev, M.S., Shavrov, V.G., et al. "Forced nonlinear precession of the second-order magnetization in a magnetoelastic material", *Journal of Communications Technology and Electronics*, **64**(1), pp. 41–51 (2019).

23. Pourreza, T., Alijani, A., Maleki, V.A., et al. "The effect of magnetic field on buckling and nonlinear vibrations of Graphene nanosheets based on nonlocal elasticity theory", *International Journal of Nano Dimension*, **13**(1), pp. 54–70 (2022).

24. Wang, Y.S. and Shih, Y.S. "Analysis of the vibration of a cracked ferromagnetic rectangular plate in a transverse magnetic field", *Journal of Vibration and Control*, **7**, 10775463221081181 (2022).

25. Li, J., Hu, Y., and Wang, Y. "The magneto-elastic internal resonances of rectangular conductive thin plate with different size ratios", *Journal of Mechanics*, **34**(5), pp. 711–723 (2018).

26. Kędzia, P., Magnucki, K., Smyczyński, M., et al. "An influence of homogeneity of magnetic field on stability of a rectangular plate", *International Journal of Structural Stability and Dynamics*, **19**(05), pp. 34–56 (2019).

27. Zhang, C., Wang, L., Eyvazian, A., et al. "Analytical solution for static and dynamic analysis of FGP cylinders integrated with FG-GPLs patches exposed to longitudinal magnetic field", *Engineering with Computers*, **56**, pp. 1–19 (2021).

28. Hosseinian, A. and Firouz-Abadi, R. "Vibrations and stability analysis of double current-carrying strips interacting with magnetic field", *Acta Mechanica*, **232**(1), pp. 229–245 (2021).

29. Firouz-Abadi, R.D. and Hosseinian, A.R. "Resonance frequencies and stability of a current-carrying suspended nanobeam in a longitudinal magnetic field", *Theoretical and Applied Mechanics Letters*, **2**(3), 031012 (2012).

30. Pourreza, T., Alijani, A., Maleki, V.A., et al. "Nonlinear vibration of nanosheets subjected to electromagnetic fields and electrical current", *Advances in Nano Research*, **10**(5), pp. 481–491 (2021).

31. Kletsel, M., Barukin, A., and Talipov, O. "About the biot-savart-laplace law and its use for calculations in high-voltage AC installations", *Electrotechnical Inspection*, **93**(11), pp. 129–132 (2017).

32. Ghaderloo, R.A., Sirat, A.P., and Shoulaie, A., *A High Frequency Active Clamp Forward Converter with Coreless Transformer*, arXiv preprint arXiv:2307, **12804** (2023). https://doi.org/10.48550/arXiv.2307.12804

33. Assadi, A. and Najaf, H. "Nonlinear static bending of single-crystalline circular nanoplates with cubic material anisotropy", *Archive of Applied Mechanics*, **90**(4), pp. 847–868 (2020).

34. Tahmasebi, E., Ashrafi Khorasani, N., and Imam, A. "Nonlinear vibration behavior of a carry current ferromagnetic beam plate under magnetic fields and thermal loads", *Journal of Vibration and Control*, **26**(15–16), pp. 1276–1285 (2020).

35. Alim A., Ngakan K., Naresh B., et al. "Multi project scheduling and material planning using lagrangian relaxation algorithm", *Industrial Engineering & Management Systems*, **20**(4), pp. 580–587 (2021).

36. Hu, Y.-D. and Xu, H.-R. "Nonlinear natural vibration of a circular plate in the non-uniform induced magnetic field", *Archive of Applied Mechanics*, **91**(6), pp. 2513–2533 (2021).

## Biographies

**Mohammadali Nasrabadi** graduated from Azad University with an MSc degree in Mechanical Engineering, Solid Mechanics, and hold his BSc from the University of Tabriz in Mechanical Engineering, Fluid Mechanics. Now, he is working as an instructor in the Department of Mechanical Engineering at the Ooj Institution of Higher Education. His research interests are solid mechanics, computation, and viscoelasticity.

**Aidin Ghaffari** graduated in Mechanical Engineering from Azad University with an MSc degree. He received his BSc degree in Mechanical Engineering, Solid Design in 2012. His research interests are sensors, renewable energy, and numerical and analytical modelling.

**Behnam Heydari** received his PhD in mechanical engineering from University of Tabriz, Tabriz, Iran. Now he is an Assistant Professor in Azad University. His research interests include computational fluid mechanics, energy systems, and heat transfer.

**Amir Afkar** received his PhD in Automotive Engineering from Iran University of Science and Technology, Tehran, Iran. Now he is working as an Assistant Professor in Technology and Engineering Research Center, Standard Research Institute, Iran. His research interests are energy, finite element method, vibration, and optimization.